مجلة العلوم البحتة والتطبيقية
Journal of Pure & Applied Sciences
www.Suj.sebhau.edu.ly ISSN 2521-9200
Received 05/08/2016 Revised 07/11/2016 Published online 16/10/2017

Low Velocity Determination based on Seismic Tomography

Naser Mohmed Elzawam
Department of Geology, Faculty of Science, Sebha University, Libya
Corresponding Author: Nas.alzawam@sebhau.edu.ly

Abstract One of the main goals in seismic data processing is to estimate seismic velocities of geological structure in the earth. Structural velocities are needed for depth migration, the process that converts seismic data, recorded as a function of time, into a depth image of subsurface. Conventional velocity analysis methods generally assume flat layered geology and mild lateral velocity variation. In areas with structurally complex geology, these methods often fail, and more sophisticated techniques are required. One of these techniques, so called seismic tomography, compares observed traveltimes, measured for each source receiver experiment, with expected traveltimes, computed by ray tracing through an assumed velocity model, the differences are projected back over the traced ray paths to produce an update to the model. The velocity-depth determination method is demonstrated on a synthetic example.

key word: Tomostatics has advantages over traditional refraction statics.

تحديد السرعة المنخفضة باستعمال أسلوب Seismic Tomography

نصر محمد الزوام
قسم علوم الأرض– كلية العلوم– جامعة سبها، ليبيا
للمراسلة: Nas.alzawam@sebhau.edu.ly

الملخص يعتبر تعين السرعة للتراكيب الجيولوجية للأرض ، احد أهداف العمليات السيزمية. حيث تكمن الحاجة لذلك من اجل عملية الارتحال العميق، وخاصة تلك العمليات التي تقوم بالانتقال من المقطع السيزمي (الزمني) وتصور المقطع الجيولوجي (العمق) التحت سطحي ، وعليه فان طرق التحليل السرعة التقليدية تأخذ في الاعتبار دائما بان الطبقات التحت سطحية في توضع افقي والتغيرات الجانبية متوسطة ، لكن في حال وجود تراكيب جيولوجية معقدة، تكون تلك الطرق عاجزة عن التعامل معها ، ولذلك تأتي الحاجة إلى أساليب تقنية متقدمة وصعبة نوعا ما، ولعل احد تلك التقنيات هي ما يعرف في الطرق السيزمية Seismic Tomography، فهي تأخذ أزمنة الانتقال المقيسة لكل مصدر و جيوفون، وبعد الحساب الزمني من خلال الأثر السيزمي، تفترض نموذج للسرعة، وفي حال وجود فرق بين ما هو حقيقيا ومتوقع، يكون هناك تعامل حسابي، ومنه يُحدث النموذج وهكذا، وعليه فان الطريقة المستعملة في هذه الورقة مستخدم فيها نماذج افتراضية.

الكلمات المفتاحية: تومو ستاتيك لها افضلية على طريقة الانكسار التقليدية.

1- INTRODUCTION:

1-1: Different Approaches to Imaging the Near Surface Velocity in Seismic Exploration

Shallow refraction seismic has long been used for the determination of the near surface layer structure. The most common goal of this investigation in seismic prospecting for gas and oil was the definition of the static corrections. The model of near surface layer was the result of refraction interpretation allowing deriving estimates of the thicknesses and velocities of the near-surface layers by analyzing the first breaks of head waves on the field records. Conventional analysis of first-break data makes use of intercept times and inverse slopes of the refracted-arrival segments of traveltime-distance graphs to interpret the depth and velocity structure of the shallow subsurface. During the last decades several different methods have been proposed for the interpretation of refraction data, such as the intercept–time method, the wavefront-reconstruction method [1] the plus-minus method [2], the general reciprocal method [3], [4], the delay time method [5]. All these methods are very useful tool of seismic interpretation and are still used to define starting model in more advanced modern interpretation techniques based on generalized linear inversion [6] or on tomographic inversion. However, all these methods have certain drawbacks restricting their range of applications. First of all they were designed only for interpretation of refraction data and it was not simple to include other types of waves (for instance reflected waves). They cannot detect velocity inversions (a low-velocity layer beneath a high-velocity) and cannot to resolve thin beds (known as the hidden layer problem). The interpretation of velocity increases with depth within a layer can be problematic with some implementations. Most of the refraction techniques were designed to compute static corrections for a constant velocity weathering layer of slowly changing thickness overlying a refractor of constant velocity. When these conditions do not exist, then unacceptable errors arise in the computed statics. To overcome these limitations new solutions based on tomographic inversion have been proposed for determination of the LVL structure and static corrections [7], [8], [9], [10], and [11]. The static corrections based on tomographic approach are named tomostatics [12] .

Tomostatics has advantages over traditional refraction statics in regions where it is not easy to identify refractors and where we can meet velocity inversion. The tomographic method enables us to consider complex geological models with dipping or variously curved layers and with strong lateral velocity variations and rough topography. Model parameterization is much more flexible. The next advantage of this method is the possibility of jointly inverting the different kinds of waves generated within a seismic experiment (turning waves, head waves, reflected waves).

The tomographic inversions may be classified from different points of view. Using different types of waves we can consider turning wave tomography, head wave tomography and reflection tomography. Tomostatics is mainly based on turning wave tomography and head wave tomography. Taking into account the theoretical principles of tomographic inversion we can distinguish between ray tomography (traveltime tomography) and diffraction tomography [13]. The main goal of the traveltime tomography is determination of the velocity distribution in the medium using propagation time of different waves [14], [15], and [16]. The main goal of the amplitude tomography is to define the attenuation distribution using amplitudes [17], [18], [19],and [20]or spectral characteristics of the waves [21], [22].

Among different types of tomography only the traveltime tomography in the variants of turning wave and head wave tomography have been widely applied to determination of the near surface velocity characteristics and statics calculations.

Different aspects of tomographic inversion applied to definition the near surface layer characteristics and static corrections were analysed in many papers.

[9]. introduced the model of LVL consisting of an undulating earth surface with a planar refracting horizon between two media divided into blocks of constant velocity. Each block was of equal horizontal length and had an unknown constant velocity. The traveltimes were computed for the waves that are refracted at the bottom of the LVL between any source and receiver locations. These traveltimes were expressed in terms of the velocities in the blocks. Testing various other models for the LVL with dipping and curved refractor boundaries did not obtain improved field static corrections on the available data. The L2 norm (smoothing technique) was used during inversion and the tomographic set of equation had typical form:

$$(\hat{A}^T\hat{A} + \lambda\hat{I})\,\Delta V = \hat{A}^T\Delta t$$

where: $\vec{I}$ - the unit matrix, $\hat{A}^T$ - transposition of coefficient matrix $\hat{A}$, λ - arbitrary parameter, ΔV - column vector of unknowns (values of velocity corrections in the nodes of computational grid), Δt - column vector of traveltime differences (measured between recorded and calculated - for assumed velocity distribution - traveltimes), $\hat{A}$ - matrix of coefficients defining relation between traveltimes and velocities.

[23].used the procedure aimed to model a laterally varying distribution of velocities and the topography of ***n*** refracting interfaces. By the specification of ***n*** vertical grid lines of equal spacing, each layer of the model is divided into a number of cells. The upper limit of the model (the surface of the earth) is specified by known elevations. The cells situated below the lower refracting interface are considered half-infinite. For each cell, a constant velocity is determined in terms of the slowness. The depths to the base of the cells, which define the refracting interfaces, are among the inversion parameters. The ray tracing procedure is developed on the concept of minimal traveltime of the first arrivals. For each station, the raypath representing the shortest traveltime of all the possible direct and refracted waves from the shot is calculated. No refraction is assumed at the vertical cell boundaries.

[24].used differences in first-arrival traveltimes between adjacent records in multifold reflection surveys to compute the depth and velocity structure of near-surface layers. The traveltime differences as a function of source-receiver offset provide a direct indication of the number of refractors present, with each refractor being defined by an offset range with a constant time difference. For each refractor, the time-difference value at a common receiver from two shotpoints is used to partition the intercept time into the delay time at each shotpoint. This procedure is repeated until the delay times at all shotpoints and for all refractors have been computed. Refractor depths and velocities are evaluated from this suite of delay times.

[25] proposed a new method for refraction statics reducing the computational time without reducing accuracy. The first arrivals, common-offset organized, formed the data space. The method involves Fourier transforming any common-offset data vector with respect to the common mid-point. As a result, the data are decomposed in a number of subspaces, associated with the wave-numbers, which can be independently inverted to obtain any wavelength of the near-surface model.

[11] investigates the feasibility of computing the weathering model from the traveltimes of refracted first arrivals. The problem is formulated in terms of the difference in arrival time at adjacent receivers, resulting in a much sparser matrix for inversion. Lateral variations in both the weathering thickness and velocity are sought. In most cases, it is necessary to include a small number of constraints to obtain the true weathering model. Any roughness in the solution that is not required to fit the data is most effectively removed using a second difference smoothing technique. Two layers make up the model: a laterally inhomogeneous weathering

layer and a uniform, high speed refractor. The weathering layer is divided into cells of constant velocity. Each cell is bounded above by the observation surface and below by the refractor. Boundaries between adjacent cells are vertical. The base of weathering is described by a series of node points, joined by straight line segments. In this study a constant refractor velocity is assumed.

[12] presented examples illustrated that turning ray tomography can image near-surface velocities more accurately than refraction statics methods. The medium to be imaged was discretized into a grid of small rectangular cells, each of which contains a single velocity. Sources and receivers are both located on the surface. The updated velocities were slightly smoothed (or damped) every few iterations. Which done by Constrained Damped Simultaneous Iterative Reconstruction Technique (CDSIRT). It was confirmed that tomostatics is noticeably closer to the true statics where velocity inversions are significant. Generally, long spatial wavelength statics appear to be estimated better using tomostatics, although a tomostatics bias (bulk shift) exists with increasing depth. Due to damping and smoothing in the tomography algorithm, the output image of a linear inversion was remarkably robust to a wide range of reasonable initial models.

[26] used turning-ray tomography for estimating near-surface velocity structure in areas where conventional refraction statics techniques fail because of poor data or lack of smooth refractor/velocity structure. The method comprises nonlinear iterations of forward ray tracing through triangular cells linear in slowness squared, coupled with the LSQR linear inversion algorithm.

[27] performed the tomography on prestack time picks using the simultaneous iterative reconstructive technique (SIRT) algorithm with modifications to include reflected as well as turned rays. Traveltimes of head waves are well approximated by rays turned in a small velocity gradient below a high contrast reflector, and so are included automatically as a special case of turned rays. The reflections, which correspond to predominantly near vertical propagation, define horizontal changes in the model, but not the vertical changes. Conversely, the turned transmissions are better able to define the vertical changes. Increasing the effective aperture by combining reflection and transmission data and performing tomography on this composite data set produces a better image of the 2-D velocity distribution.

[28] presented a nonlinear refraction traveltime tomography method that consists of a new version of the shortest path ray-tracing approach , a regularized nonlinear inversion method that inverts “traveltime curves” rather than traveltimes alone, and a Monte Carlo method for nonlinear uncertainty analysis of the final solution. Seismic raypaths were defined by calculating the shortest traveltime paths through a network consisting of nodes and representing the earth. They chose to solve an inverse problem that explicitly minimizes data misfit as well as model roughness.

[10] developed a new algorithm for tomographic inversion of traveltimes of reflected and refracted seismic waves. In the case of a very inexact initial model, a ‘layer-by-layer’ inversion strategy was recommended as a first inversion step. It was assumed that the model consists of several layers separated by interfaces represented by a set of points connected by straight segments. Velocity distribution in each layer was described by means of its own velocity grid, the layer being completely inside the grid. The velocity values were specified at gridnodes; bilinear interpolation was used in between them.

[29] introduced considerable factors which effect the resolution and accuracy result of tomostatics based on turning wave.

[7] used a joint inversion of both first and refracted arrivals in order to obtain a well-resolved velocity field for the computation of static corrections. After the analysis of the diving waves, they inverted the traveltimes associated with the refracted events by using the velocity model obtained from the diving waves as the initial model. Also after inverting the two refracted arrivals separately they used the resulting output velocity field as a new initial model for jointly inverting again the direct arrivals and the traveltimes with the first and second refracted waves, in order to obtain a more accurate velocity field in depth.

[8] analysed the applications of refraction statics and tomostatics on test lines. For longer deeper anomalies with irregular raypaths, refraction statics and tomostatics were expected to provide major improvements; however, only marginal improvements were observed. In the test line considered the refraction statics provided the best section visually in terms of signal strength, sharpness and continuity, with a structure that seems geologically reasonable. The image provided by tomostatics was similar in structure, but was much noisier. However, only the tomostatics solution was able to focus some events in the most difficult area.

2- Material and Methods

2- 1: Quantitative Evaluation:

For the purpose of quantitative evaluation of the inversion effectiveness the following errors were calculated:

$$RMSE = \left(\frac{\sum_{i=1}^{R} \left(V_{i,est} - V_{i,\mathrm{mod}} \right)^2}{R} \right)^{1/2}$$

$$RMSDT = \left(\frac{\sum_{i=1}^{N} \left(t_{i,est} - t_{i,\mathrm{mod}} \right)^2}{N} \right)^{1/2}$$

Where:

$V_{i,est}$ – the value of velocity estimated in the i – th node,

$V_{i,mod}$ – the known value of model velocity in the i – th node,

R – the number of nodes in the velocity grid,

$t_{i,est}$ – the traveltime for i – th ray calulated for the velocity field estimated in the inversion process,

$t_{i,mod}$ – the observed (known from seismic modeling) traveltime for i-th ray,

N – the number of considered seismic rays

Both of first error RMSE and the second error RMSDT estimate using(Fortran90), and bitmaps of resulting velocity fields as well as the difference between assumed model velocity fields and resulting from inversion presented (using Surfer 9 Software)

Before tomographic inversion the refractor in starting models is removed and the layer below is replaced by the medium with velocity equal to the velocity a little above the refractor. This was done to avoid the effect of layer below refractor on behaving rays a little above the refractor. As a result all the velocity fields resulting from inversion do not include refractor and do not include the layer below the refractor.

2-2- Synthetic Data Example

The two layer model with gradient medium over refractor

In order to validate seismic tomography can improve the resloution of the inversion result , desired a simple near surface model as shownin figure (1). In the first layer the velocity increase linearly as depth increse, the velocity of first layer $(V_1 = 960 + 4 * h(m/s))$over half-space with constant velocity $(3500m/s)$,where (h) refere as depth in (m)The depth of the refractor is 176 m. Aditionaly in the first layer the velocity anomaly is placed with the following parameters: depth varied from (48-80 m), width 12 CDP's (300 m), velocity 800 m/s. The velocity in the first layer is incresing from 960 m/s near surface to 1670 m/s near refractor. This starting model was modified through changing anomaly velocity from 800 m/s to 600 m/s and 400 m/s for the case of low velocity anomaly. The dimensions of the velocity cell were 1 CDP (25 m) in the horizontal direction and 8 m in the vertical direction.

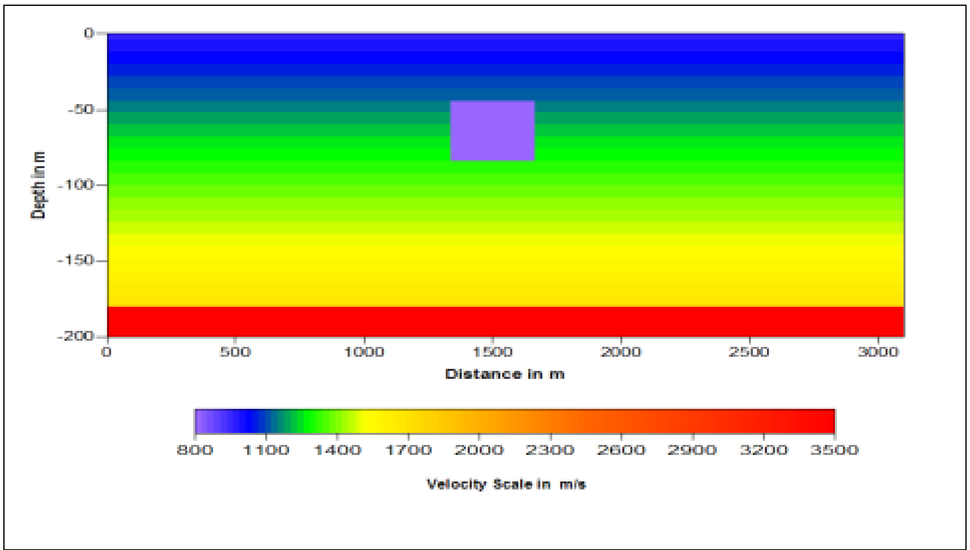

Fig. 1. Two layer velocity model with velocity anomaly and gradient medium over constant velocity half-space, refractor depth 176 m

The parameters used for calulations of traveltimes and ray trajectories had the following values: positions of shots 1000 and 2000 m, receiver interval 50m, spread of 24 geophones. The example of ray trajectories for velocity anomaly 600 m/s are presented in fig. 2.

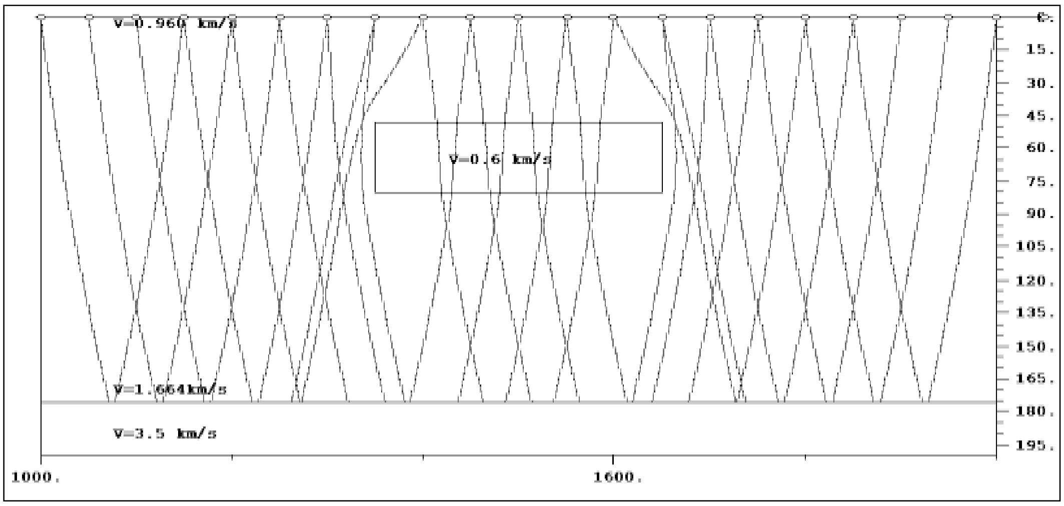

Fig. 2. Part of the ray trajectories for the model with velocity anomaly 600 m/s, 2 shot points, refractor depth 176 m; horizontal axis – distance in m, vertical axis – depth in m

In the next figures 3 –7 the results of tomographic inversions are presented for anomaly velocity 400 m/s, refractor depth 176 m and for different iteration number. The position of assumed anomaly is marked as white rectangle. For the starting velocity model the traveltime error RMSDT was equal 33.28 ms.

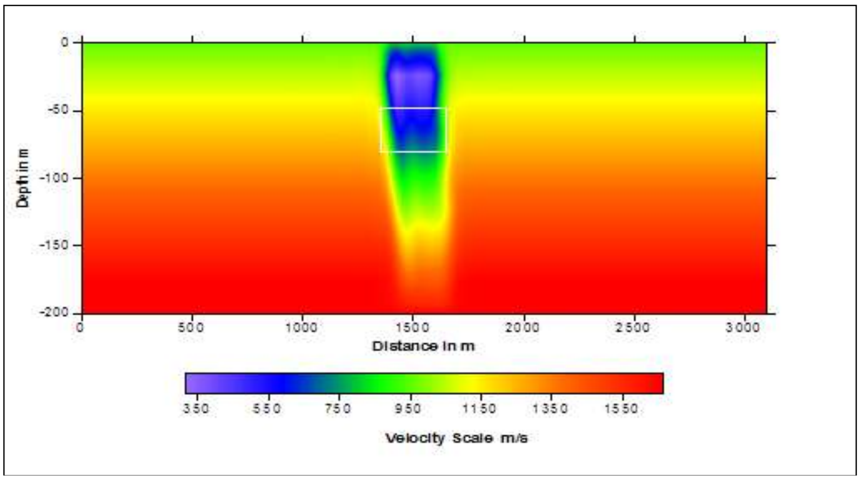

Fig. 3. The result of inversion in 1-st iteration (without smoothing) in the case of anomaly velocity 400 m/s (RMSDV= 122 m/s , RMSDT= 17.90 ms)

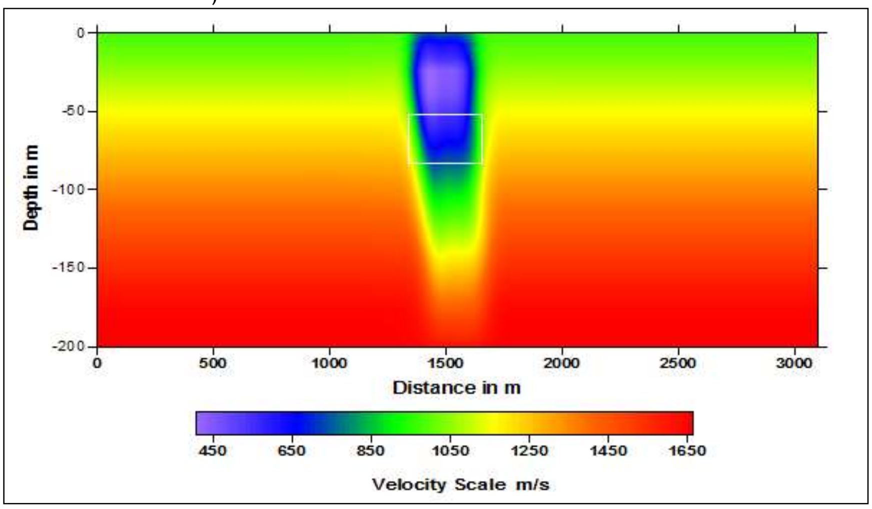

Fig. 4. The result of inversion in 1-st iteration after smoothing in the case of anomaly velocity 400 m/s (RMSDV=124 m/s).

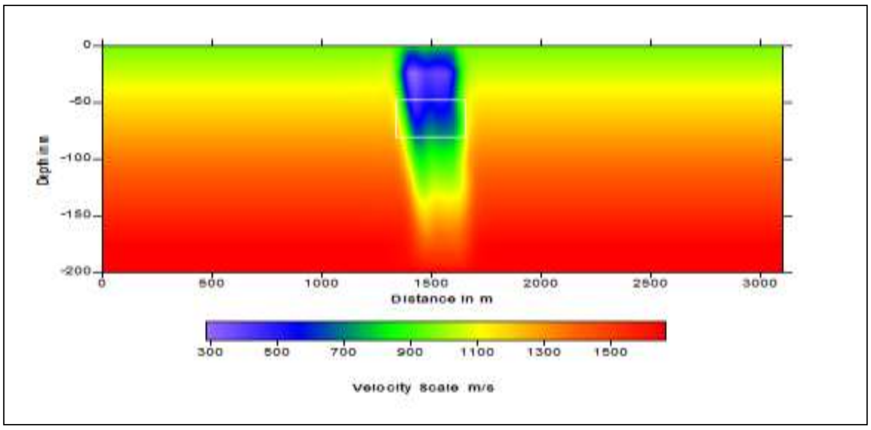

Fig. 5. The result of inversion in 2-nd iteration (without smoothing) in the case of anomaly velocity 400 m/s (RMSDV=124 m/s, RMSDT=1.19 ms)

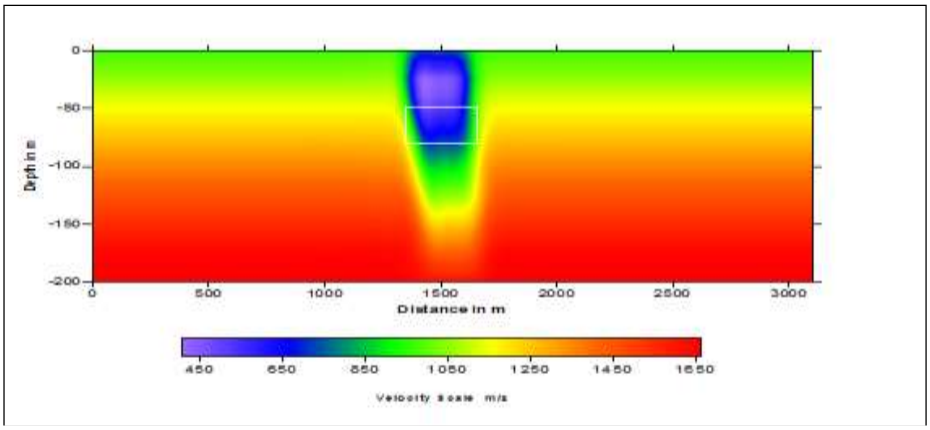

Fig. 6. The result of inversion in 2-nd iteration (with smoothing after 1-st iteration) in the case of anomaly velocity 400 m/s (RMSDV= 119 m/s)

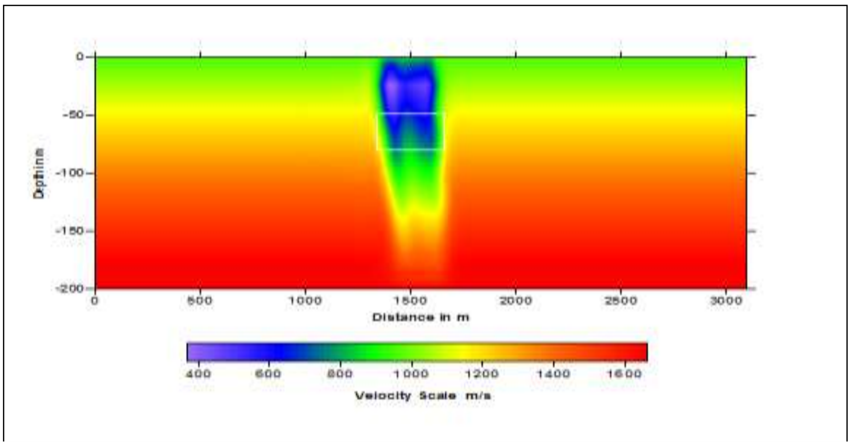

Fig. 7. The result of inversion in 3-nd iteration (without smoothing after 2-st) in the case of anomaly velocity 400 m/s (RMSDV=117 m/s, RMSDT=0.33 ms)

The results of statics calculations for different iterations in the case of anomaly velocity 400 m/s are presented below.

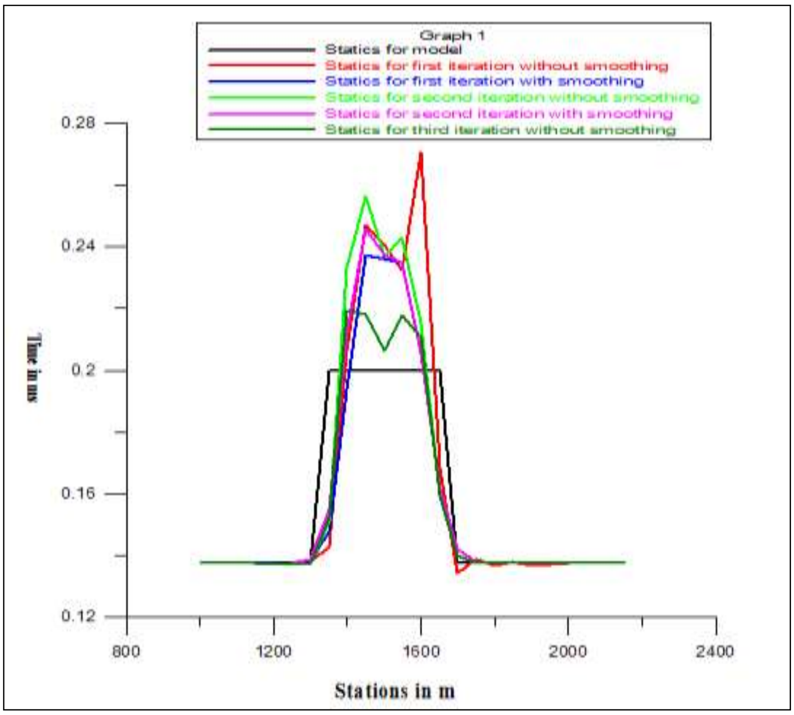

Fig. 8. The results of statics calculations for different iterations in the case of anomaly velocity 400 m/s, refractor depth 176 m

In the next figures 9 – 12 the results of tomographic inversions are presented for anomaly velocity 600 m/s, refractor depth 176 m and for different iteration number.

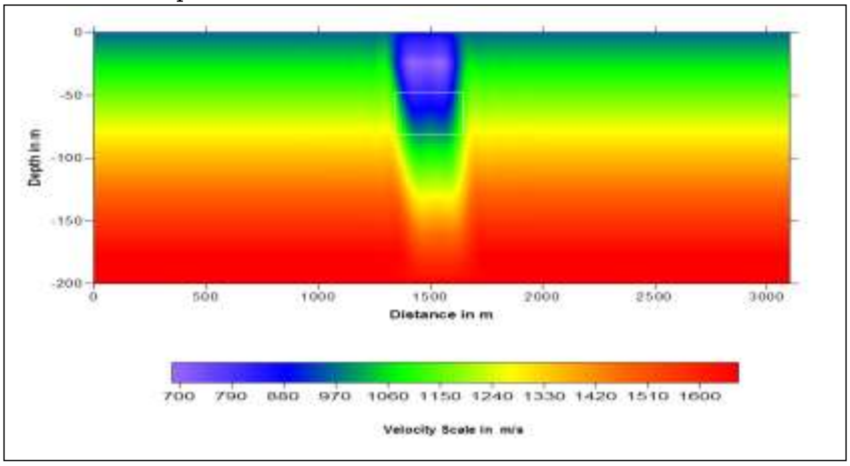

Fig. 9. The result of inversion in 1-st iteration (without smoothing) in the case of anomaly velocity 600 m/s (RMSDV= 80 m/s , RMSDT= 2.85 ms)

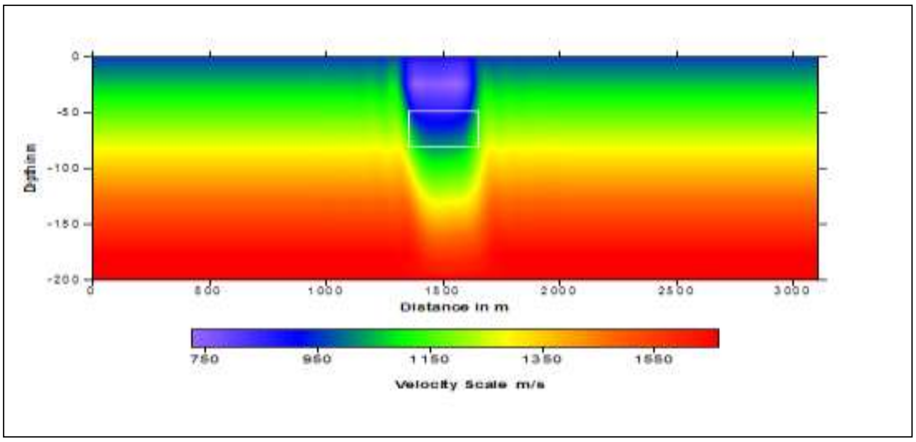

Fig. 10. The result of inversion in 2-nd iteration (without smoothing) in the case of anomaly velocity 600 m/s (RMSDV=79 m/s, RMSDT=0.33 ms)

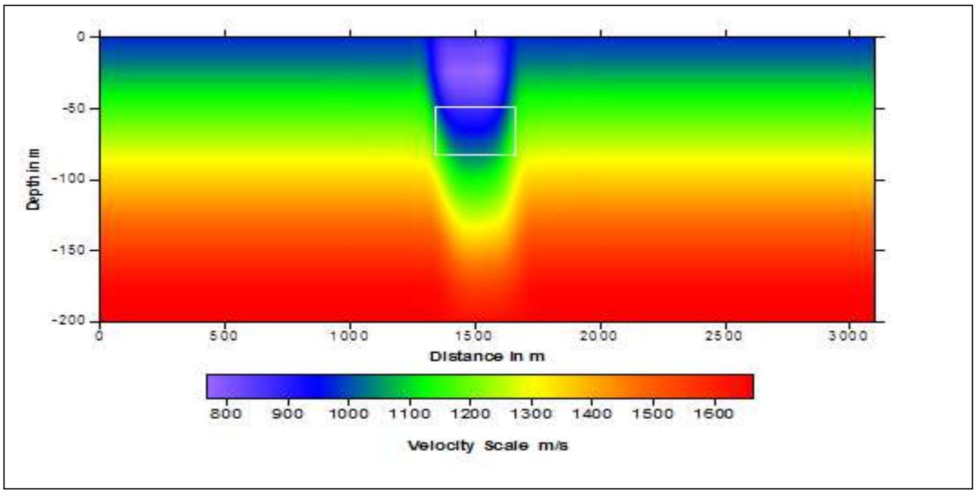

Fig. 11. The result of inversion in 2-nd iteration (with smoothing after 1-st) in the case of anomaly velocity 600 m/s (RMSDV=79 m/s)

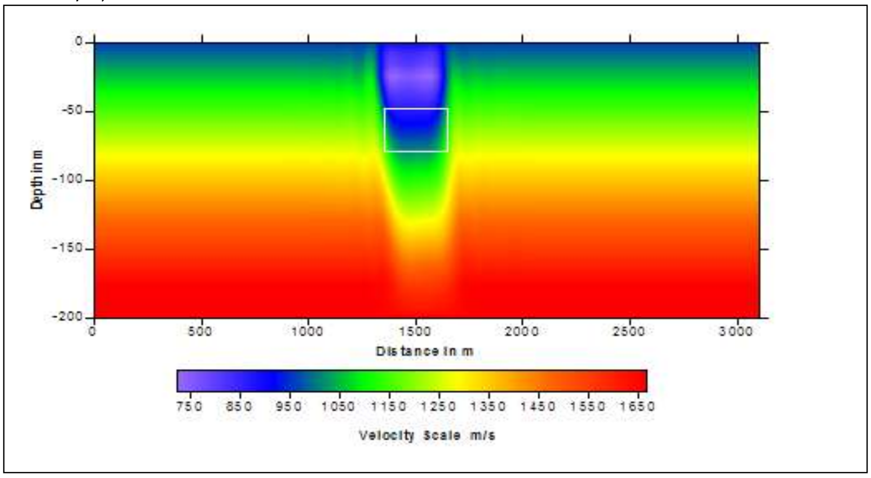

Fig. 12. The result of inversion in 3-nd iteration (without smoothing after 2-nd iteration) in the case of anomaly velocity 600 m/s (RMSDV=79 m/s, RMSDT=0.03 ms

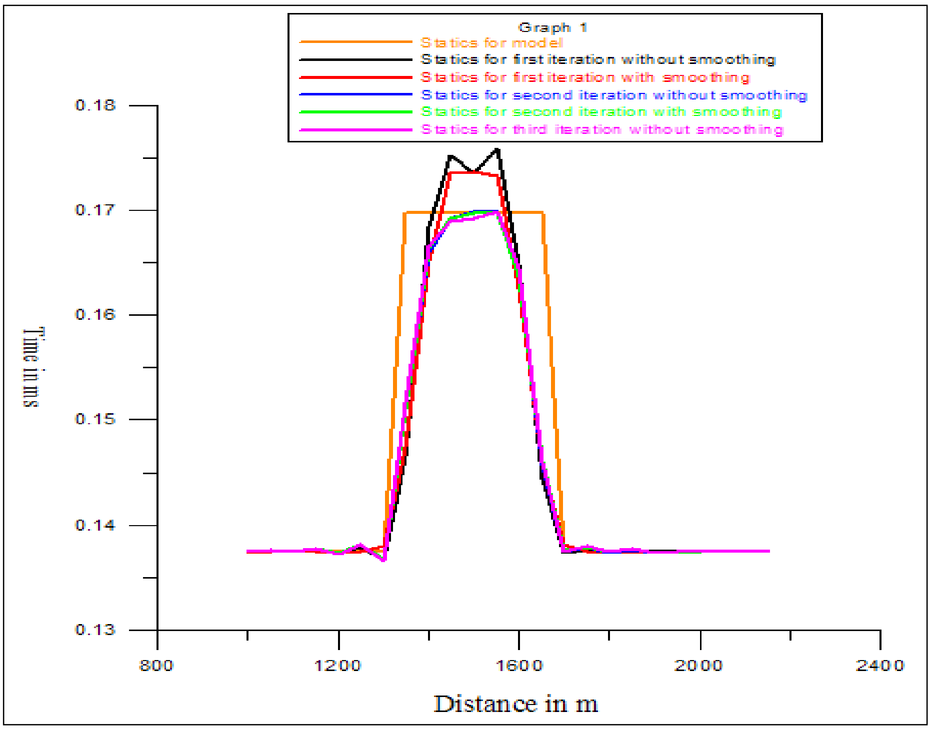

Fig. 13. The results of statics calculations for different iterations in the case of anomaly velocity 600 m/s, refractor depth 176 m

In the next figures 14-17 the results of tomographic inversions are presented for anomaly velocity 800 m/s, refractor depth 176 m and for different iteration number.

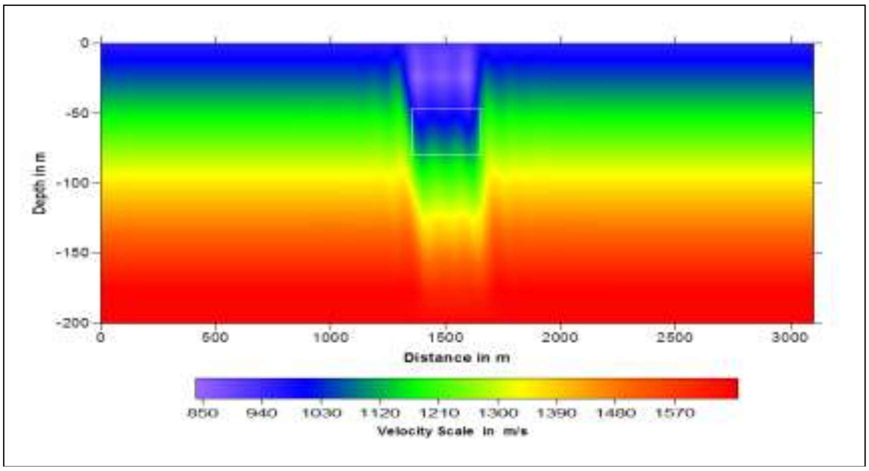

Fig. 14. The result of inversion in 1-st iteration (without smoothing) in the case of anomaly velocity 800 m/s (RMSDV= 53 m/s , RMSDT= 0.88 ms)

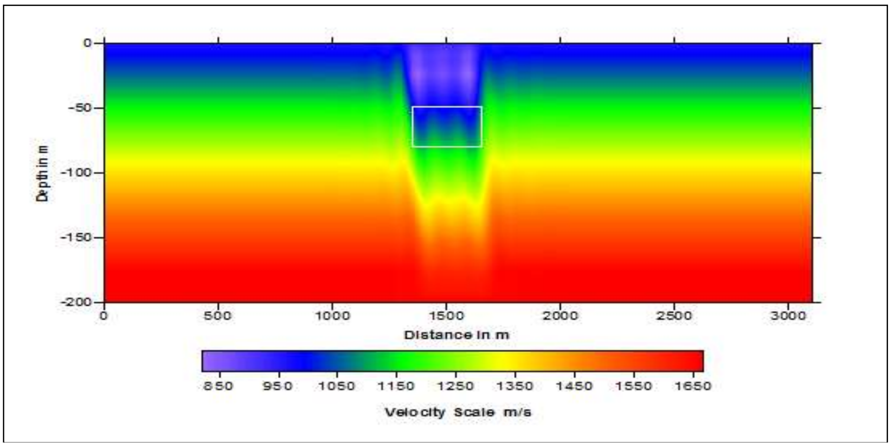

Fig. 15. The result of inversion in 2-nd iteration (without smoothing) in the case of anomaly velocity 800 m/s (RMSDV=53 m/s, RMSDT=0.08 ms).

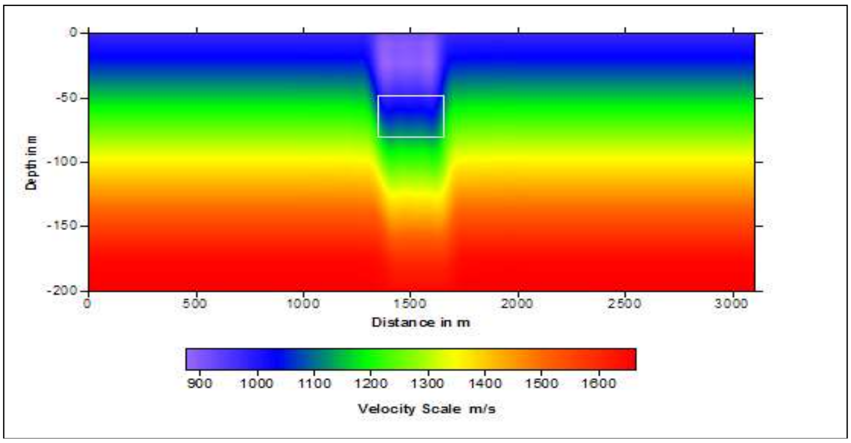

Fig. 16. The result of inversion in 2-nd iteration (with smoothing after 1-st) in the case of anomaly velocity 800 m/s (RMSDV=52 m/s)

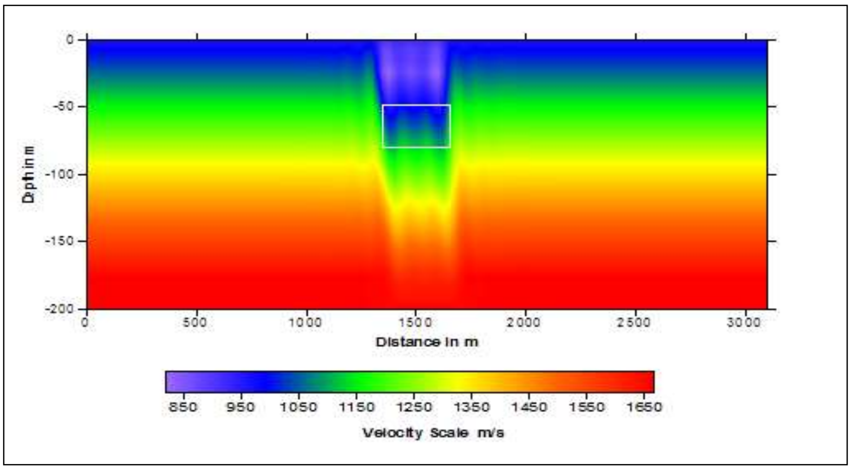

Fig. 17. The result of inversion in 3-nd iteration (without smoothing after 2-st) in the case of anomaly velocity 800 m/s (RMSDV= 53 m/s, RMSDT= 0.01 ms)

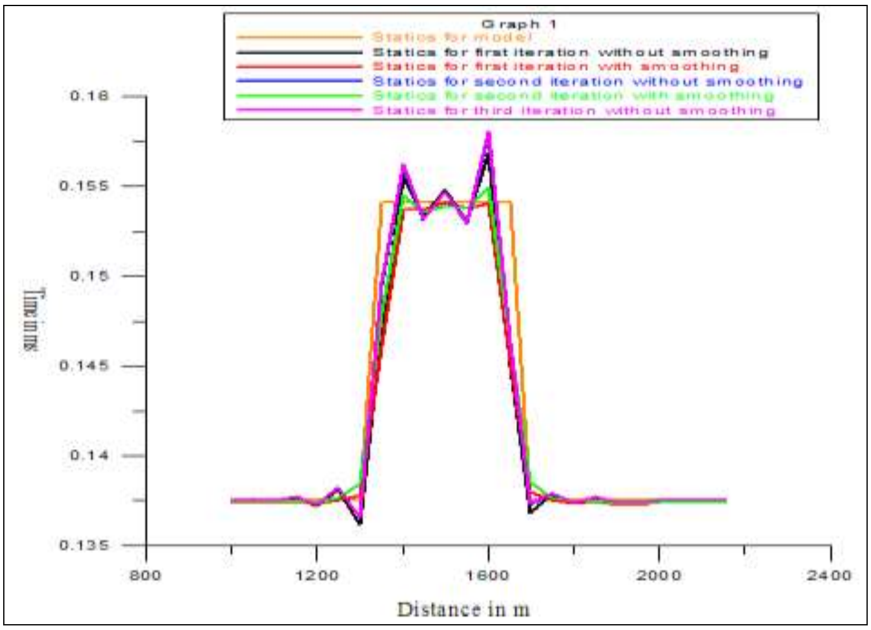

Fig. 18. The results of statics calculations for different iterations in the case of anomaly velocity 800 m/s, refractor depth 176 m

Table 1. The values of RMSDV (m/s) for different values of anomaly velocity and for different options of smoothing application

Anomaly velocity (m/s)	Starting Values	First Iteration	Second iteration Without smoothing	Second iteration With smoothing	Third iteration without smoothing
400	129	126	124	119	117
600	81	80	79	79	79
800	55	53	53	52	53

Table 2. The values of RMDT (ms) for different values of anomaly velocity and for different number of iterations

Anomaly velocity (m/s)	Starting Values	First iteration without smoothing	Second iteration without smoothing	Third iteration without smoothing
400	33.88	17.90	1.19	0.33
600	16.88	2.85	0.31	0.03
800	10.06	0.88	0.08	0.01

3- Results and Conclusion

The resulting from the analysis defines the effectiveness of statics estimation by means of tomographic inversion of first breaks. It was confirmed that for the discussed models of low velocity layer the head wave tomography based on first breaks inversion of typical land records may be treated as an effective tool of field statics estimation although the vertical resolution of resulting velocity fields is relatively very weak, but horizontal resolution is very good. Although the proper depth cannot be define of anomaly, we can estimate quit well its horizontal position. Additionally we can observe very interesting compensation effect in vertical direction: decreasing of velocity in one zone (connected with low velocity anomaly) is compensated by increasing of velocity outside this zone (below and above). Thanks to this compensation effect the static corrections – defined as always for vertical propagation of rays – are in all cases estimated with good accuracy if several iterations of tomographic inversion is applied and proper spatial smoothing of velocity field is done. Additionally the analysed approach may be applied not only to the gradient models of low velocity layer like in the case of turning ray tomography.

It was quit enough to estimate statics but not enough to identify the velocity anomalies. The solution to this problem may be to use simultaneously head wave tomography and turning ray tomography. Of course such a solution may be applied only in case of gradient layers.

REFRENCES:

[1]- Thornburgh H.R. 1930 - Wavefront diagrams in seismic interpretation. *AAPG Bulletin* 14, 185-200.

[2]- Hagedoorn J.G., 1959 - The plus-minus method of interpreting seismic refraction sections. *Geophysical Prospecting*, vol. **7**, 158–182

[3]- Palmer, D. 1980 - *The Generalized Reciprocal Method of Seismic Refraction Interpretation,* K. B. *S* . Burke (ed.). SEG, Tulsa

[4]- Palmer. D., 1981 - An introduction to the generalized reciprocal method of seismic refraction interpretation. *Geophysics*, 46, 1508-1518

[5]- Barry K. M., 1967- Delay time and its application to refraction profile interpretation. *Seismic Refracting Prospecting,* Musgrave (ed.), 348-361. SEG, Tulsa.

[6]- Hampson, D., and Russell B., 1984 - First-break interpretation using generalized linear inversion. J*. Can. Soc. Expl. Geophys.*, vol. 20, 40-54

[7]- Bohm G., Accaino F., Rossi G. and Tinivella U., 2006 - Tomographic joint inversion of first arrivals in a real case from Saudi Arabia, Section I – Madrid Workshop on Near-Surface 2005. *Geophysical Prospecting,* 2006, vol. 54, 721–730

[8]- Bridle R., Barsoukov N, Al-Homaili M., Ley R. and Al-Mustafa A., 2006 - Comparing state-of the art near-surface models of a seismic test line from Saudi Arabia, Section I –Madrid Workshop on Near-Surface 2005, *Geophysical Prospecting,* 2006, vol. 54, 667–680

[9]- De Amorim M, Hubral W.N., P. and Tygel, M., 1987 - Computing Field Statics with the Help of Seismic Tomography. *Geophysical Prospecting*, vol. 35, 907-919

[10]- Ditmar P., Penopp J., Kasig R. and Makris J., 1999 - Interpretation of shallow refraction seismic data by reflection/refraction tomography. *Geophysical Prospecting*, 1999, vol. 47, 871–901

[11]- Docherty P., 1992 - Solving for the thickness and velocity of the weathering layer using 2-D refraction tomography. *Geophysics*, vol. 57, no. 10, 1307-1318

[12]- Zhu X., Sixta, D. P., Angstman, B. G., 1992 - Tomostatics: Turning-ray tomography + static corrections. *The Leading Edge,* 11, no. 12, 1

[13]- Tura M., Greaves R., Beydoun W.,Inderwiesen, Lo 1994 - Crosswell seismic reflection/diffraction tomography: A reservoir characterization application. *Geophysics*, vol. 59, 351-361

[14]- Scott P. W. and Fehler M. C., 1991 - Traveltime tomography: A comparison of popular methods. *Geophysics*, vol. 56, no. 10, 1639-1649

[15]- Michelena R. J., 1993 - Singular value decomposition for cross-well tomography. *Geophysics*, vol. 58, 1655-1661

[16]- Michelena R. J., Muir F., Harris J. M., 1993 - Anisotropic traveltime tomography. *Geophysical Prospecting*, vol. 41, 381-412

[17]- Brzostowski M., McMechan G., 1992 - 3-D tomographic imaging of near-surface seismic velocity and attenuation. *Geophysics*, vol. 57, 396-403

[18]- Liao Q., McMechan G. A., 1997 - Tomographic imaging of velocity and Q, with application to crosswell seismic data from the Gypsy Pilot Site, Oklahoma. *Geophysics*, vol. 62, 1804-1811

[19]- Neep J. P., Sams M. S., Worthington M. H., O'Hara-Dhand K. A., 1996 - Measurement of seismic attenuation from high-resolution crosshole data. *Geophysics*, vol. 61, 1175-1188

[20]- Leggett M., Goulty N.R. and Kragh J.E., 1993 - Study of traveltime and amplitude time-lapse tomography using physical model data. *Geophysical Prospecting*, vol. 41, 599-619.

[21]- Quan Y., Harris J. M., 1997 - Seismic attenuation tomography using the frequency shift method. *Geophysics*, vol. 62, 895-905

[22]- Chris L., Hackert and Parra J. O., 2004 - Improving Q estimates from seismic reflection data using well-log-based localized spectral correction.*Geophysics*, vol. 69, no. 6, 1521–1529

[23]- Olsen K. B., 1989 - A stable and flexible procedur for the inverse modeling of seismic first arrivals. *Geophys. Prosp.*, vol. 37, 455-465

[24]- Lawton D. C., 1989 - Computation of refraction static corrections using first-break traveltime differences. *Geophysics*, vol. 54, 1289–1296

[25]- Zanzi L and Carlini A. 1991 - Refraction statics in the wavenumber domain. *Geophysics*, vol. 56, no. 10, p. 1661-1670.

[26]- Stefani J. P., Joseph P. 1995 - Turning-ray tomography. *Geophysics*, vol. 60, no. 6, 1917-1929

[27]- Rajasekaran S. and McMechan G. A., 1996 - Tomographic estimation of the spatial distribution of statics. *Geophysics*, vol. 61, no. 4, 1198-1208

[28]- Zhang J. and Toksöz M. N., 1998 - Nonlinear refraction traveltime tomography. *Geophysics*, no. 5, 1726-1737.

[29]- Zhu X. 2002 - Velocity imaging through complex near-surface structures by tomography. E37, EAGE 64th Conference & Exhibition — Florence, Italy, 27 - 30 May 2002